CYBERNETICS AND PHYSICS, VOL. 14, NO. 3, 2025, 275–284

TRAJECTORY CONTROL OF QUADCOPTER USING F-PID CONTROLLER UNDER DISTURBANCES AND UNCERTAINTIES

Arpit Sharma
Electrical Engineering Department
National Institute of Technology,
Kurukshetra, India
arpit_62100018@nitkkr.ac.in
(Corresponding author)

Narender Saini
School of Engineering and Technology
CGC University, Mohali-140307,
Punjab, India
narendersaini7379@gmail.com

Jagdeep Singh Lather
Electrical Engineering Department
National Institute of Technology,
Kurukshetra, India
jslather@nitkkr.ac.in

Article history:
Received 24.09.2025, Accepted 20.11.2025

Abstract

Trajectory control of quadcopters becomes important for their operations in hazardous environments as well as pandemic-hit areas. This becomes intricate due to the complicated dynamics of the quadcopter in the face of disturbances and parameter uncertainties. PID control and Fuzzy control are inherently robust due to their model-free nature. This paper aims to control the altitude and rotational angles of a 6-DoF (degree of freedom) quadcopter using a hybrid Fuzzy-PID (F-PID) controller, followed by an analysis of the designed controller under disturbances and parametric uncertainty. The designed controller improves the quadcopter dynamics by maintaining its trajectory in uncertain and disturbed environmental conditions. The 6-DoF quadcopter model, along with the proposed hybrid F-PID controller, has been simulated in MATLAB®. Furthermore, the proposed F-PID controller and conventional PID controller performances have been compared in terms of critical parameters such as rising time, settling time, peak overshoot, and steady state error.

Key words

Quadcopter, Proportional–Integral- Derivative controller, F-PID controller, Disturbances, Uncertainty.

1 Introduction

The quadcopters are being used for mission-critical transportation, operations in hazardous environments like Covid-19 hit areas, agriculture farms, cinematography, logistics in congested localities, area surveillance for law and order etc. around the world [Idrissi et al., 2022; Sharma and Lather, 2024]. The quadcopter trajectory control in such applications becomes a challenging task due to the presence of disturbances and parameter fluctuations as well [Kumar and Dewan, 2024]. The quadcopter model is intricate due to high nonlinearity and strongly coupled translational and rotational motions [Amin et al., 2016]. Although quadcopters are widely deployed across applications such as aerial photography, surveillance, and logistics, obtaining an accurate dynamic model becomes challenging in tasks involving rapid maneuvers, disturbance-affected outdoor flight, variable payloads, and precise trajectory tracking. These conditions introduce strong nonlinearities and parameter variations, making both model building and control design difficult [Luchinsky et al.,]. Such situations make it extremely difficult to control quadcopters while they are hovering [Kumar and Dewan, 2020; Al-Younes et al., 2010]. Model-free PID controllers have been designed to operate quadcopters for stable operations without overshoot/ sustained oscillations [Sabzevari et al., 2016]. To enhance responsiveness, model-based linear quadratic controller (LQR) and model predictive controller have been designed for quadcopters [Ahmad et al., 2020; Ribeiro et al., 2015]. However, such model-based controllers are extremely sensitive to parameter variations to an extent to admits unacceptable behaviour with minor changes in system parameters. In practice, no system is ideal; there is always some uncertainty present in the nonlinear model. Likewise, quadcopters are also subjected to disturbances and uncertainty [Bellahcene et al., 2021]. To solve this problem, the authors in [Kumar and Dewan, 2022a; Modirrousta and Khodabandeh, 2015] have proposed a nonlinear sliding mode controller (SMC) and a backstepping controller. Further to improve the performance of the quadcopter, extended SMCs are developed, such as adaptive SMC, second-order SMC and integral backstepping SMC [Luque-Vega et al., 2012; Nguyen et al., 2021]. A fuzzy logic controller is also an alternative, which is

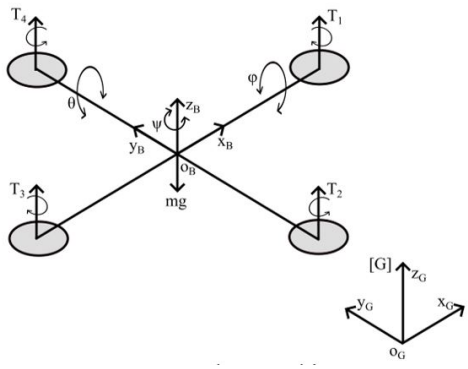

Figure 1: Quadcopter Model

simple but effective against the disturbances and uncertainty [Zaeri et al., 2019]. Further hybridization of the fuzzy logic controller with the PID controller is more effective as compared to conventional PID as well as the fuzzy logic controller. When there is a wind disturbance, the F-PID controller gives better results compared to a conventional PID controller [Kuantama et al., 2017]. Different kinds of controllers have been designed, which focus mainly on different fuzzy logic controllers like Mamdani and Sugeno fuzzy logic controllers and concluded that the Mamdani fuzzy controller in the hybridization with the PD controller gives the best results among these controllers [Leal et al., 2021]. In this paper, different kinds of disturbances such as Aerodynamic factor, external noise, sensor noise and wind effect (WE) as well as parametric uncertainty have been considered with the quadcopter model and solved this quadcopter model with the help of an F-PID controller to get the better results. From the rotational angle part, only roll and pitch have been controlled in this paper, yaw has not been controlled because, in conventional control, it does not make any big impact on the trajectory tracking of the quadcopter, so it can be ignored. The introduction of the quadcopter and formulation of the problems which are associated with the quadcopter are covered in Section 1 of this paper. The mathematical dynamics of the quadcopter and disturbances with their modelling are covered in Section 2. Section 3 provides the suggested control strategy used for the quadcopter model. The results and discussion are illustrated in Section 4, and then there are the conclusions in Section 5.

2 Quadcopter Model

The quadcopter, as a rigid-body mechanical system, has six degrees of freedom. The motion within these degrees of freedom is actuated by varying the speeds of the four propellers. Speed combinations of propellers decide what trajectory the quadcopter will follow. There are several important parameters in a quadcopter which help us understand the dynamics of the quadcopter. Also, these parameters play an important role in directly controlling the trajectory of the quadcopter. These parameters are called rotational and translational parameters. The quadcopter's position is defined by using the coordinates x(East), y(North) and z(Up) and also indicate the distance from the point of origin, which is fixed to the earth and known as the inertial reference frame. ϕ and θ angles are used to represent the rotational angles with respect to body frame reference of the quadcopter [Usman,]. In this work, it has been assumed that the quadcopter is a rigid body whose motion is described using two coordinate frames: an inertial earth-fixed frame $\mathbf{G} = [o_B, x_G, y_G, z_G]$.and a body-fixed frame $\mathbf{B} = [o_B, x_B, y_B, z_B]$ attached to the centre of mass of the quadcopter. The relationship between these two frames is illustrated in Fig. 1 [Aisuwarya et al.,].

In many earlier studies, the dynamics model of the underactuated quadcopter has been presented and used. Let ϕ, θ, ψ denote the roll, pitch, and yaw angles, respectively.

The rotors' angular speeds can be combined to regulate the quadcopter's position in space. Four lift forces $F_i (i = 1, 2, 3, 4)$ are generated by the four rotors. The quadcopter's translational motion, $P_G = [x, y, z]'_G$, is described by the E-frame. Where z is the vertical position and positions in the horizontal plane is x and y. Rotational motion, i.e. Euler angles $Q_B = [\phi, \theta, \psi]'_B$ are described by the B-frame. The following rotation matrix, which makes use of Euler angles, illustrates how the quadcopter rotates from its body to its earth frame [Runcharoon and Srichatrapimuk, 2013] concerning the ground $R_{B\to G}(Q) \in R^{3\times 3}$.

$$R_{B\to G}(Q) = \begin{bmatrix} c\theta c\psi & s\phi s\theta c\psi - c\phi s\psi & c\phi s\theta c\psi + s\phi s\psi \\ c\theta s\psi & s\phi s\theta s\psi + c\phi c\psi & c\phi s\theta s\psi - s\phi c\psi \\ -s\theta & s\phi c\theta & c\phi c\theta \end{bmatrix} \tag{1}$$

Angular transformation (T_A) of equation 1 is given by:

$$T_A = \begin{bmatrix} 1 & s\phi t\theta & c\phi t\theta \\ 0 & c\phi & -s\phi \\ 0 & s\phi se\theta & c\phi se\theta \end{bmatrix} \tag{2}$$

Where, s, c, se and t stands for $\sin, \cos, \sec$ and $\tan$, respectively.

Scenario 1 It has been assumed that the quadcopter model [Le et al., 2018] is free from the disturbances.

$$\begin{cases} \ddot{x} = (\cos\phi \sin\theta \cos\psi + \sin\phi \sin\psi)\dfrac{u_1}{m} \\ \ddot{y} = (\cos\phi \sin\theta \sin\psi - \sin\phi \cos\psi)\dfrac{u_1}{m} \\ \ddot{z} = -g + (\cos\phi \cos\theta)\dfrac{u_1}{m} \\ \ddot{\phi} = \dot{\theta}\dot{\psi}\dfrac{J_y - J_z}{J_x} + \dfrac{l}{J_x}u_2 + \dfrac{J_r}{J_x}\dot{\theta}\Omega_r \\ \ddot{\theta} = \dot{\phi}\dot{\psi}\dfrac{J_z - J_x}{J_y} + \dfrac{l}{J_y}u_3 - \dfrac{J_r}{J_y}\dot{\phi}\Omega_r \\ \ddot{\psi} = \dot{\phi}\dot{\theta}\dfrac{J_x - J_y}{J_z} + \dfrac{1}{J_z}u_4 \end{cases} \tag{3}$$

Scenario 2 The quadcopter's mathematical model when there are disturbances

$d_i^{ext} \to (i = x, y, z, \phi, \theta, \psi), (d_i^{ext} > 0)$ and uncertainty of +20% and -20% is;

$$\begin{cases} \ddot{x} = (\cos\phi \sin\theta \cos\psi + \sin\phi \sin\psi)\dfrac{U_1}{m \pm \Delta m} + d_x^{ext} \\ \ddot{y} = (\cos\phi \sin\theta \sin\psi - \sin\phi \cos\psi)\dfrac{U_1}{m \pm \Delta m} + d_y^{ext} \\ \ddot{z} = -g + (\cos\phi \cos\theta)\dfrac{U_1}{m \pm \Delta m} + d_z^{ext} \\ \ddot{\phi} = \dot{\theta}\dot{\psi}(\dfrac{(J_y - J_z)}{J_x} + \dfrac{l}{J_x}u_2 + \dfrac{J_r}{J_x}\dot{\theta}\tau_r + d_\phi^{ext} \\ \ddot{\theta} = \dot{\phi}\dot{\psi}\dfrac{(J_z - J_x)}{J_y} + \dfrac{l}{J_y}u_3 - \dfrac{J_r}{J_y}\dot{\phi}\tau_r + d_\theta^{ext} \\ \ddot{\psi} = \dot{\phi}\dot{\theta}\dfrac{(J_x - J_y)}{J_z} + \dfrac{1}{J_z}u_4 + d_\psi^{ext} \end{cases} \tag{4}$$

Here, disturbances are defined as;

$$d_i^{ext} = d_i^{ad} + d_i^{en} + d_i^{wn} + d_i^{sn} \tag{5}$$

Where, d_i^{ad} represents aerodynamic factor which includes air friction and drag factor and has been concluded in [Kumar and Dewan, 2022b],

$$d_i^{ad} = \sin(2t) \tag{6}$$

d_i^{en} represents external noise, which is different for z and ϕ, θ, is given in [Le et al., 2018];

$$\begin{cases} d_z^{\text{en}}(t) &= 18 + 4\cos\left(\dfrac{\pi t}{6}\right) \\ d_\phi^{\text{en}}(t) = d_\theta^{\text{en}}(t) &= 7 + 2\cos\left(\dfrac{2\pi t}{3}\right) \end{cases} \tag{7}$$

d_i^{sn} shows sensor noise, which is represented by a random number signal from MATLAB® library with mean value 0, variance 0.0001 and sample time 0.01 and d_i^{wn} represents wind noise which is used as a shock wave from 10 seconds to 12 seconds. The Velocity of wind noise is considered as 3 m/s. Uncertainty in the model leads to the variation in the quadcopter's weight by 20%. The dynamic mathematical quadcopter model includes J_x (about x-axis), J_y (about y-axis) and J_z (about z-axis) which are inertias whereas, J_r represents the inertia of motor and τ_r represents angular velocity of rotor.

$$\mathbf{z} = \begin{vmatrix} z_1, z_2, z_3, z_4, z_5, z_6, \\ z_7, z_8, z_9, z_{10}, z_{11}, z_{12} \end{vmatrix}^T$$

$$= \begin{vmatrix} \phi, \dot{\phi}, \theta, \dot{\theta}, \psi, \dot{\psi}, \\ z, \dot{z}, x, \dot{x}, y, \dot{y} \end{vmatrix}^T \in \mathbb{R}^{12}$$

$$\mathbf{u} = \begin{vmatrix} u_1, u_2, u_3, u_4 \end{vmatrix}^T$$

Definitions of these and other parameters as well as their values have been taken from [Sharma and Lather, 2025]. Total thrust about the z-axis acting on the body is equal to $U_1 \propto (F_1 + F_2 + F_3 + F_4)$, $U_2 \propto (-F_2 + F_4)$ and $U_3 \propto (-F_1 + F_3)$ are roll and pitch inputs, respectively; and $U_4 \propto (-F_1 + F_2 + F_3 + F_4)$ is the yaw moment [Fang et al., 2010]. Here $F_i (i = 1, 2, 3, 4)$ represents force induced by propellers, b stands for the lift coefficient, d stands for drag coefficient and $s_i (i = 1, 2, 3, 4)$ represents propeller speeds.

$$u = \begin{bmatrix} u_1 \\ u_2 \\ u_3 \\ u_4 \end{bmatrix} = \begin{bmatrix} b(s_1^2 + s_2^2 + s_3^2 + s_4^2) \\ b(s_4^2 - s_2^2) \\ b(s_3^2 - s_1^2) \\ d(s_2^2 + s_4^2 - s_1^2 - s_3^2) \end{bmatrix} \tag{8}$$

And the total residual angular speed of motors (s_r) can be written as,

$$s_r = -s_1 + s_2 - s_3 + s_4 \tag{9}$$

3 Control Design

A controller is crucial to the correct operation of a quadcopter. The quadcopter will be unstable without a controller. There are several algorithms and control techniques, however, in this project, a feedback control system using a PID controller and F-PID controller is used. The main goal of the controller is to keep the quadcopter system stable and track the reference trajectories. The mathematical model given by equation 3 [Xiong and Zheng, 2014a; Bouabdallah et al., ebb4] can be expressed in state-space form as follows:

$$\dot{Z} = f(Z, u) \tag{10}$$

Where Z and u represent state vector and input vector respectively,

$$\dot{Z} = \begin{cases} \dot{z_1} = z_2 \\ \dot{Z_2} = a_1 z_4 z_6 + a_2 z_4 \tau_r + b_1 u_2, y \\ \dot{z_3} = z_4 \\ \dot{z_4} = a_3 z_2 z_6 + a_4 z_2 \tau_r + b_2 u_3 \\ \dot{z_5} = z_6 \\ \dot{z_6} = a_5 z_2 z_4 + b_3 u_4 \\ \dot{z_7} = z_8 \\ \dot{z_8} = \dfrac{1}{m}(c z_1 c z_3) u_1 - g \\ \dot{z_9} = z_{10} \\ \dot{z_{10}} = \dfrac{1}{m} u_x u_1 \\ \dot{z_{11}} = z_{12} \\ \dot{z_{12}} = \dfrac{1}{m} u_y u_1 \end{cases} \tag{11}$$

where,

$$\begin{cases} \left[\, z_1 \; z_3 \; z_5 \,\right]^{\mathsf{T}} \in R^3 = \left[\, \phi \; \theta \; \psi \,\right]^{\mathsf{T}}, \\ \left[\, z_2 \; z_4 \; z_6 \,\right]^{\mathsf{T}} \in R^3 = \left[\, \dot{\phi} \; \dot{\theta} \; \dot{\psi} \,\right]^{\mathsf{T}}, \end{cases}$$

$$\begin{cases} a_1 = \dfrac{(J_y - J_z)}{J_x}, \qquad a_3 = \dfrac{(J_z - J_x)}{J_y}, \\ a_5 = \dfrac{(J_x - J_y)}{J_z}, \qquad a_2 = \dfrac{J_r}{J_x}, \qquad a_4 = -\dfrac{J_r}{J_y}, \\ b_1 = \dfrac{1}{J_x}, \qquad b_2 = \dfrac{1}{J_y}, \qquad b_3 = \dfrac{1}{J_z}, \\ u_x = cz_1 sz_3 cz_5 + sz_1 sz_5, \\ u_y = cz_1 sz_3 sz_5 - sz_1 cz_5, \end{cases} \tag{12}$$

It is noted that the input vector corresponds to the equivalent collective thrust and body torques acting on the quadcopter. In practical implementation, these inputs are generated indirectly through the rotor angular speeds, which serve as the actual actuators. The use of thrust and torque as virtual control inputs is a standard simplification in control-oriented quadcopter models, as rotor dynamics are significantly faster than the rigid-body dynamics, and the mapping from rotor speeds to these inputs is well established. This abstraction allows clearer control design without affecting the validity of the comparative analysis. According to [Xiong and Zheng, 2014b], the quadcopter dynamics are strongly coupled and nonlinear. There are simply four control inputs and six output variables in the quadcopter system. Fig. 2 depicts a controller's system for systematic control.

3.1 Proportional-Integral-Derivative (PID) Controller

A PID controller is an example of a feedback control system, which continually calculates the error as the difference between a desired set point and the actual process variable. In order to move the process variable closer to the desired set point, the controller subsequently modifies the process control input depending on the error value [Usman,]. Three key parts constitute the PID controller: Proportional Control: This control action is exactly proportional to the error between the set point and the process variable. The controller responds fast to changes in the process variable since its output is directly proportional to the error signal. Integral Control: The action is proportional to the time integral of the error signal. The integral action continuously modifies the controller's output to guarantee that the steady-state error is reduced over time, assisting in its elimination. Derivative Control: The rate of change of the error signal is proportional to this control action. The derivative action helps to dampen the response of the controller by predicting the future behaviour of the process variable and adjusting the output of the controller accordingly. The combination of these three components allows the PID controller to regulate the process variable in a precise and stable manner. The controller gains and time constants are tuned to achieve the desired performance of the control system. There is also a built-in PID block in MATLAB® Simulink, which also does the tuning by itself, by linearizing the model. To adjust the actual values acquired from the plant model in accordance with the desired input values, a PID-based controller is used. There are three PIDs altogether, for altitude, roll and pitch.

3.1.1 PID Tuning A common tuning technique in control systems to establish the parameters of a PID controller is the Ziegler-Nichols approach. The Ziegler-Nichols method involves performing step tests on the system and analyzing the response to determine the controller parameters. The following are the steps involved in the Ziegler-Nichols method: Step 1: Initially, the proportional gain is adjusted while keeping the derivative and integral gains at zero until the system begins to oscillate around the desired setpoint. The specific proportional gain value at which the system exhibits oscillations is referred to as the ultimate gain, and the corresponding oscillation period is termed the ultimate period. Step 2: Determine the values of K_u and T_u, use them to calculate the proportional, integral, and derivative gains of the PID controller according to Table 1:

Table 1: Ziegler-Nichols Tuning parameters

Controller Type	K_P	T_I	T_D
P	0.5 K_u	0	0
PI	0.45 K_u	T_u/1.2	0
PID	K_u/1.7	T_u/2	T_u/8

Implement the PID controller with the calculated gains and perform further tests to evaluate its performance. Adjust the gains as necessary to achieve the desired response. A PID controller is used in this work, so from this paper's perspective, only the PID controller's gain values are required and forget the P and PI controllers. The equation for the PID controller looks like:

$$U(t) = K_P e(t) + K_I \int_0^t e(t)dt + K_D \frac{de(t)}{dt} \tag{13}$$

Where K_P, K_I, K_D represent proportional gain, integral gain, and derivative gain respectively. Error value denoted by $e(t)$ and $U(t)$ represents PID control variable. Error $e(t)$ further defines as; $e(t) =$ desired value - actual value

3.1.2 F-PID Controller The F-PID controller is a combination of two different controllers, one is a Fuzzy

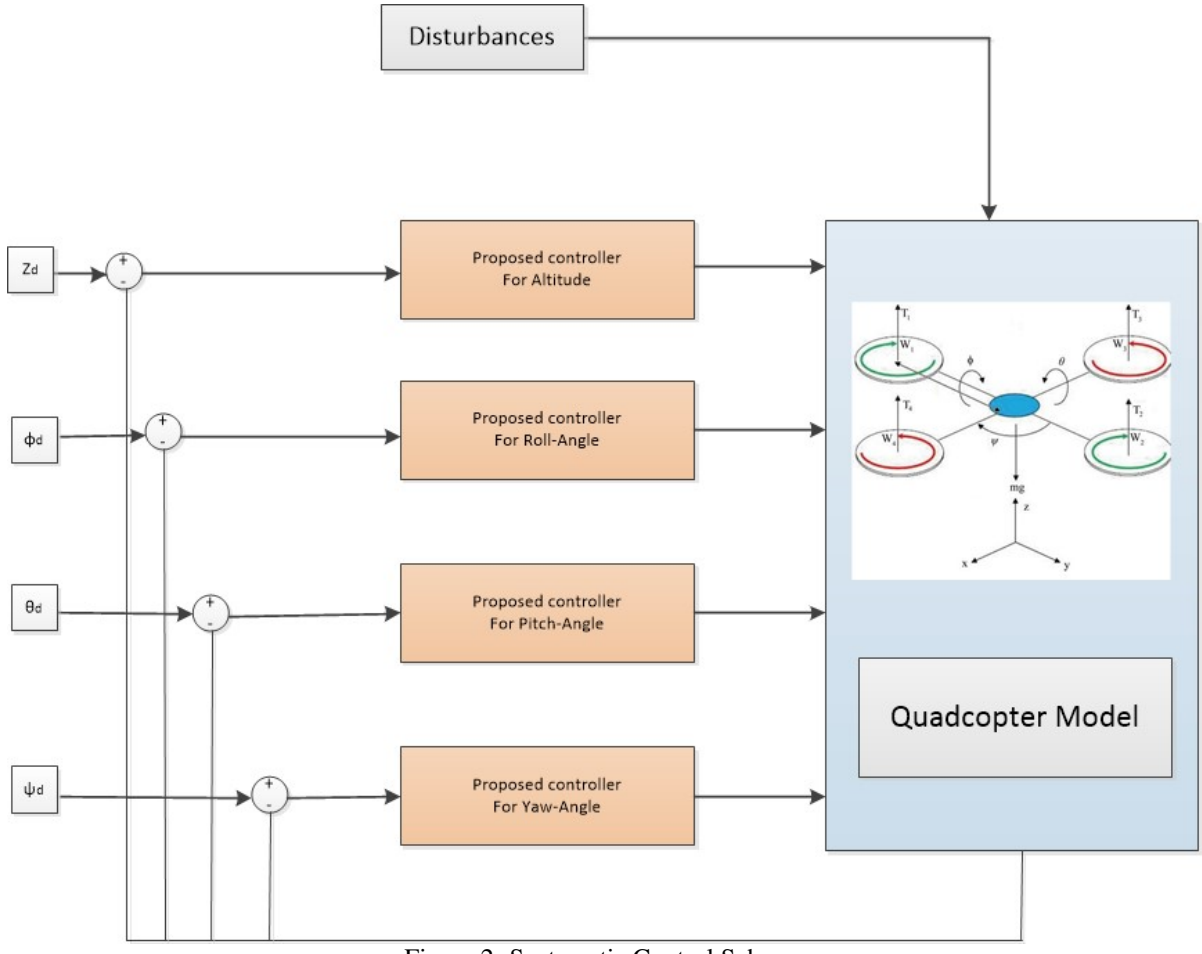

Figure 2: Systematic Control Scheme

logic controller (FLC) and the other is a PID controller. Gains are generated using FLC to reduce start-up volatility. There are 25 possible rules in FLC because each input uses five linguistic variables, using all possible input combinations. The set of linguistic values includes negative big (NB), negative small (NS), zero (ZE), positive small (PS), and positive big (PB) for two inputs and two outputs with 25 rules. With two inputs and two outputs, a Mamdani type with triangle membership functions is used. Inputs for the same are e and δe, whereas outputs are ΔK_P and ΔK_I. The FLC uses MIN for the operation of the t-norm and MAX for the operation of the s-norm. MIN is used for implication, Centroid for defuzzification and MAX is used for aggregation [Rabah et al., 2018]. All the 25 If-Then interference rules have been shown in 2, and the rule surfaces which are the same for both are shown in Fig. 3.

F-PID control algorithms employ pre-specified good Fuzzy rules to modify the parameters to the maximum time to meet the various self-tuning parameter requirements; therefore, it is crucial to create appropriate Fuzzy rules for the UAV's position control. In this F-PID controller, K_P stands for the scale factor. By increasing the value of K_p, the desired angular velocity of the four-rotor aircraft can be brought closer to the actual angular velocity, improving the accuracy of the system's adjustment. This improves the accuracy of the system's adjustment. The UAV's steady-state inaccuracy will be eliminated by raising the integral coefficient K_I.

Table 2: If-Then interference rules for K_p and K_i

Error / (δe / δt)	NB	NS	ZE	PS	PB
NB	NB	NB	NB	NS	ZE
NS	NB	NB	NS	ZE	PS
ZE	NB	NS	ZE	PS	PB
PS	NS	ZE	PS	PB	PB
PB	ZE	PS	PB	PB	PB

The membership of the inputs and outputs is shown in Fig. 4.

4 Simulation and Results

Two different kinds of controllers (PID and F-PID) have been implemented on a quadcopter, and the results of rotational angles and altitude using both the controllers (PID and F-PID) in the absence and presence of disturbances and uncertainty. SIMULINK toolbox of

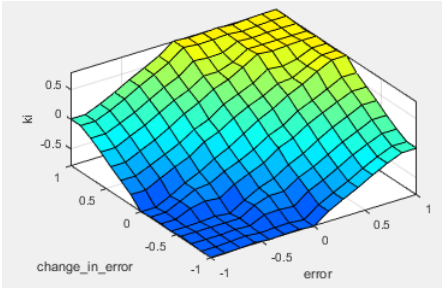

(a)

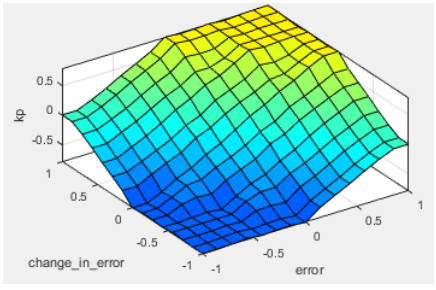

(b)

Figure 3: Fuzzy Rule surface, (a) For $\Delta K_I, (b) For \Delta K_P$

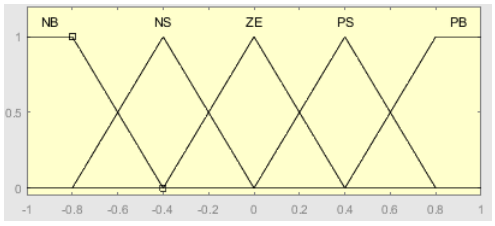

(a)

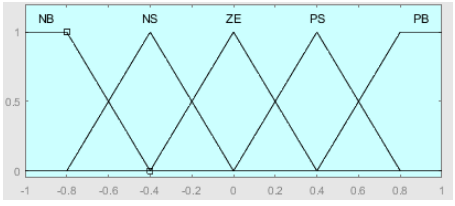

(b)

Figure 4: (a) F-PID input membership functions. (b) F-PID output membership function.

MATLAB® version 2021a license, NIT Kurukshetra has been used for simulations. The desired value for altitude is 1 meter, and for roll and pitch values are 0.2 degrees for both. Simulation has been carried out for 20 seconds. Desired values are the same for both controllers to observe which controller is best suitable to the given conditions. Different performance specifications of the PID Controller and F-PID controller have been mentioned in Table 4 and Table 6 , respectively, with the help of results obtained for a better understanding.

4.1 PID Controller

This controller has been used for two different scenarios which are following.

Scenario 1 This section represents the response and comparison of quadcopter without any disturbance $d_i^{ext} = 0$, with the help of PID controller.

4.1.1 Altitude PID Tuning Tune the values of P, I and D as mentioned in section 3.1. Following several alterations and fixes, the completely tuned PID produced the results which are shown in Fig. 5 (a) for the mathematical model which has no disturbance. The outcomes are very pleasing; in less than 10 seconds, the quadcopter stabilizes at a height of 1 meter. The PID gain of a tuned altitude PID controller is displayed in Table 3. The same objectives can be completed in even less time, but the quadcopter will act aggressively.

4.1.2 Roll (Phi) and Pitch (Theta) PID Tuning PIDs for roll and pitch have the same gain levels and responses since they operate on the same principle. Fig. 5 (b and c) depicts the quadcopter's roll or pitch reaction when the desired angle is 0.2 degrees, and the quadcopter is attempting to achieve that angle. The PID gains of a tuned roll and pitch PID controller are displayed in Table 3.

Table 3: Gain values for F-PID controller for scenario 1 and scenario 2.

Parameters	Altitude	Roll	Pitch
Kp	8	0.48	0.030
Ki	7	0.000012	0.000012
Kd	5.1	0.055	0.05

Scenario 2 This section represents the response and comparison of quadcopter in the presence of disturbance $d^{tot} \neq 0$ and uncertainty of ±20% as mentioned in section 2 with the help of PID controller. PID tuning is done for rotational angles and altitude as similar to scenario 1 and gain values are same as the scenario 1. Results have been shown in Fig. 6 for both rotational angles and altitude. The values of all the critical aspects related to control system has been calculated and tabled in Table 4.

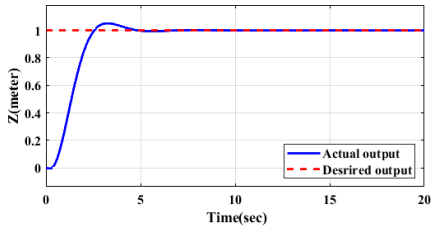

(a)

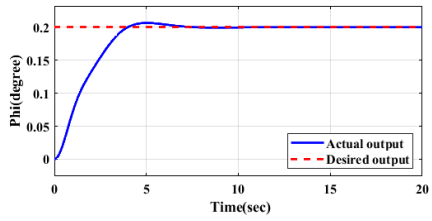

(b)

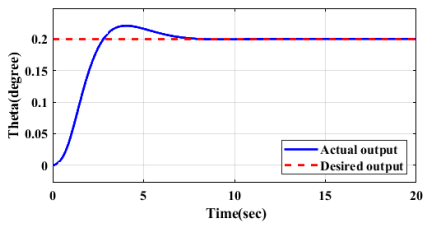

(c)

Figure 5: Responses (without disturbances and uncertainty) while using PID controller. (a) Altitude, (b) Phi, (c) Theta

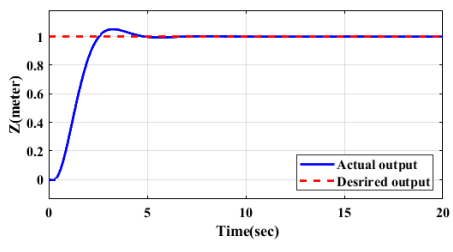

(d)Altitude

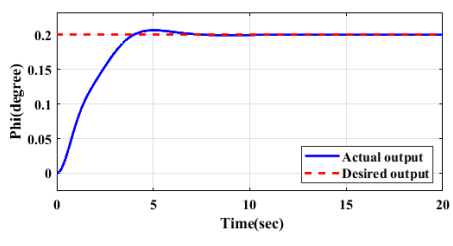

(e)Phi

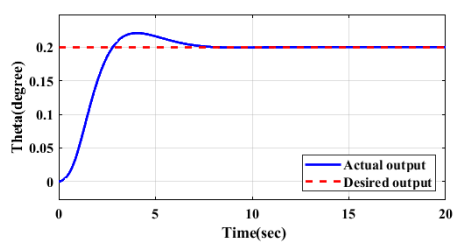

(f)Theta

Figure 6: Responses (with disturbances and uncertainty) using PID controller (a) Altitude (b) Phi (c) Theta

Table 4: Performance Specifications with PID controller

Parameters			**z**	ϕ	θ
Peak Overshoot Value	Scen.-1	No WE	0.052	0.005	0.018
	Scen.-2	No WE	0.049	0.029	0.043
		WE	0.202	0.182	0.217
		No WE+20% PU	0.027	0.028	0.039
		No WE-20% PU	0.087	0.033	0.040
		WE+20% PU	0.167	0.182	0.217
		WE-20% PU	0.281	0.182	0.217
Peak Overshoot Time	Scen.-1	No WE	3.421	5.052	3.983
	Scen.-2	No WE	3.712	3.682	4.451
		WE	14.113	11.551	11.821
		No WE+20% PU	3.512	3.621	4.443
		No WE-20% PU	3.851	3.752	4.482
		WE+20% PU	14.163	11.550	11.810
		WE-20% PU	14.182	11.552	11.812
Settling Time	Scen.-1	No WE	5.521	7.612	7.910
	Scen.-2	No WE	5.552	6.921	10.152
		WE	16.782	17.514	17.753
		No WE+20% PU	5.621	6.851	9.423
		No WE-20% PU	5.983	6.914	9.983
		WE+20% PU	16.671	17.352	17.912
		WE-20% PU	16.692	17.521	17.930
Rise Time	Scen.-1	No WE	1.534	2.736	1.719
	Scen.-2	No WE	0.872	1.565	1.622
		WE	0.869	1.569	1.601
		No WE+20% PU	1.094	1.597	1.589
		No WE-20% PU	0.682	1.557	1.630
		WE+20% PU	1.077	1.596	1.587
		WE-20% PU	0.679	1.531	1.621
Steady State Error	Scen.-1	No WE	0.0001	0.0001	0.0001
	Scen.-2	No WE	0.0003	0.0130	0.0268
		WE	0.0005	0.0140	0.0230
		No WE+20% PU	0.0010	0.0140	0.0270
		No WE-20% PU	0.0005	0.0130	0.0250
		WE+20% PU	0.0022	0.0140	0.0230
		WE-20% PU	0.0001	0.0140	0.0230

4.2 F-PID Controller

Like the previous controller, F-PID controller is also used for two different scenarios. **Scenario 1** This section represents the response of quadcopter without any disturbance $d_i^{ext} = 0$ and uncertainty with the help of F-PID controller. The output values (ΔK_p and ΔK_i) of fuzzy controller when the inputs are error (difference between actual value and desired value) and differentiation of error have been achieved with the help of MATLAB®. Further, to improve the results, PID gain values have been added to the fuzzy controller outputs. The values of the PID gains have been shown in Table 5. With the help of rotational angles and altitude results, rise time, overshoot time, settling time and steady state error have been achieved and shown in Table 6 and the results (Altitude, Roll and Pitch) for the same are shown in Fig. 7. **Scenario 2** This section represents the response of quad-

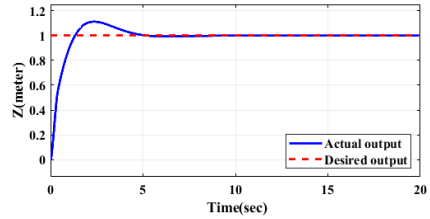

(a)

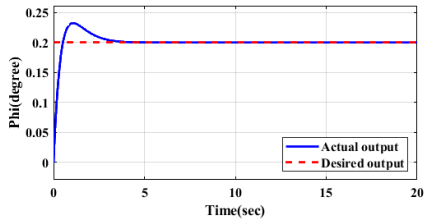

(b)

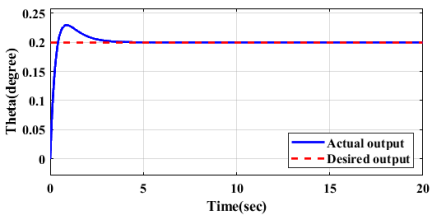

(c)

Figure 7: Responses (without disturbances and uncertainty) while using F-PID controller. (a) Altitude, (b) Phi, (c) Theta

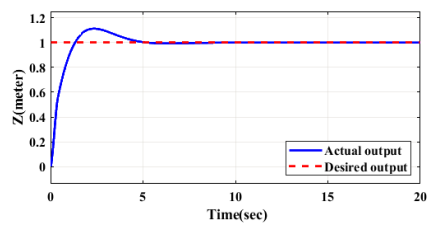

(a)

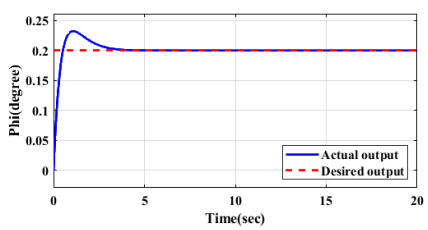

(b)

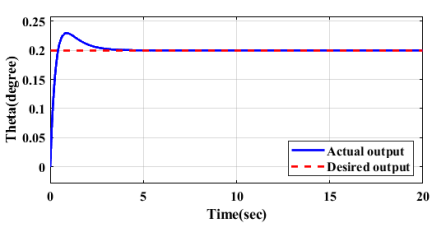

(c)

Figure 8: Responses (with disturbances and uncertainty) while using F-PID controller. (a) Altitude, (b) Phi, (c) Theta

copter in the presence of disturbance $d^{tot} \neq 0$ and uncertainty of 20% with the help of F-PID controller. The rotational angles and altitude results of quadcopter in the presence of disturbances and uncertainty are achieved as similar to scenario 1 and shown in Fig. 8. And the rise time, overshoot time, settling time and steady state error have been shown in Table 6 to understand the behavior of quadcopter model with the help of results achieved.

Table 5: Gain values for F-PID controller for scenario 1 and scenario 2.

Parameters	Altitude	Roll	Pitch
Kp	50	42	45
Ki	39	38	44
Kd	34	12	10

Table 6: Performance Specifications with F-PID controller

Parameters			**z**	ϕ	θ
Peak Overshoot Value	Scen.-1	No WE	0.113	0.027	0.025
	Scen.-2	No WE	0.067	0.032	0.029
		WE	0.067	0.032	0.029
		No WE+20% PU	0.059	0.032	0.029
		No WE-20% PU	0.081	0.032	0.029
		WE+20% PU	0.059	0.032	0.029
		WE-20% PU	0.081	0.032	0.029
Peak Overshoot Time	Scen.-1	No WE	2.350	1.130	0.930
	Scen.-2	No WE	3.253	1.080	0.880
		WE	3.251	1.080	0.880
		No WE+20% PU	3.520	1.085	0.890
		No WE-20% PU	3.012	1.085	0.890
		WE+20% PU	3.522	1.080	0.890
		WE-20% PU	3.023	1.085	0.890
Settling Time	Scen.-1	No WE	5.314	5.112	4.821
	Scen.-2	No WE	6.224	5.641	5.314
		WE	15.426	14.211	13.721
		No WE+20% PU	6.452	5.648	5.322
		No WE-20% PU	5.963	5.612	5.298
		WE+20% PU	15.432	14.224	13.736
		WE-20% PU	15.411	14.205	13.715
Rise Time	Scen.-1	No WE	0.908	0.414	0.327
	Scen.-2	No WE	1.602	0.382	0.308
		WE	1.602	0.380	0.314
		No WE+20% PU	1.577	0.381	0.312
		No WE-20% PU	1.405	0.382	0.313
		WE+20% PU	1.750	0.381	0.312
		WE-20% PU	1.405	0.382	0.310
Steady State Error	Scen.-1	No WE	0.0002	0.0001	0.0001
	Scen.-2	No WE	0.0001	0.0001	0.0001
		WE	0.0002	0.0001	0.0001
		No WE+20% PU	0.0001	0.0002	0.0001
		No WE-20% PU	0.0002	0.0001	0.0002
		WE+20% PU	0.0003	0.0001	0.0001
		WE-20% PU	0.0002	0.0001	0.0001

From the outcomes, it has been seen that the PID controller and F-PID controller are almost equally effective when there are no disturbances and uncertainty present in the quadcopter model, but after the introduction of disturbances in the system, the PID controller does not work efficiently, whereas the F-PID controller easily handles disturbances and gives much better results. Further, after introducing the uncertainty in the quadcopter model, it has been seen that uncertainty does not make any noticeable change in roll and pitch trajectories, whereas in altitude, uncertainty effect has been seen easily.

5 Conclusion

In this paper, a hybrid Fuzzy logic controller with a Proportional-Integral-Derivative controller is proposed to eliminate the effect of different kinds of disturbances and uncertainty in the system. Performance of the proposed controller has been proven by simulation in MATLAB software and compared with the performance of the Proportional-Integral-Derivative controller. The quadcopter tracks the reference trajectories (rotational angles and altitude) with the help of the proposed F-PID controller and ensures that the system does not lose its stability in different conditions. The proposed methodology has successfully tracked the quadcopter's rotational angles and altitude movement to the desired/reference quantity for a finite period, even when there are disturbances and uncertainty in the system.

References

Ahmad, F., Kumar, P., Bhandari, A., and Patil, P. P. (2020). Simulation of the quadcopter dynamics with lqr based control. *Materials Today: Proceedings*, **24**, pp. 326–332.

Aisuwarya, R., Yonas, F. M., and Yendri, D.

Al-Younes, Y. M., Al-Jarrah, M. A., and Jhemi, A. A. (2010). Linear vs. nonlinear control techniques for a quadrotor vehicle. In *ISMA'10 - 7th International Symposium on Mechatronics and its Applications*, pp. 1–10.

Amin, R., Aijun, L., and Shamshirband, S. (2016). A review of quadrotor uav: Control methodologies and performance evaluation. *International Journal of Automation and Control*, **10** (2), pp. 87–103.

Bellahcene, Z., Bouhamida, M., Denai, M., and Assali, K. (2021). Adaptive neural network-based robust h tracking control of a quadrotor uav under wind disturbances. *International Journal of Automation and Control*, **15** (1), pp. 28–57.

Bouabdallah, S., Murrieri, P., and Siegwart, R. (200ebb4). Design and control of an indoor micro quadrotor. In *IEEE International Conference on Robotics and Automation (ICRA)*, vol. 5, pp. 4393–4398.

Fang, Z., Wang, X. Y., and Sun, J. (2010). Design and nonlinear control of an indoor quadrotor flying robot. In *Proceedings of the World Congress on Intelligent Control and Automation (WCICA)*, pp. 429–434.

Idrissi, M., Salami, M., and Annaz, F. (2022). A review of quadrotor unmanned aerial vehicles: Applications, architectural design and control algorithms. *Journal of Intelligent and Robotic Systems*, **104** (2).

Kuantama, E., Vesselenyi, T., Dzitac, S., and Tarca, R. (2017). Pid and fuzzy-pid control model for quadcopter attitude with disturbance parameter. *International Journal of Computers, Communications & Control*, **12** (4), pp. 519–532.

Kumar, S. and Dewan, L. (2020). Different control scheme for the quadcopter: A brief tour. In *2020 1st IEEE International Conference on Measurement, Instrumentation, Control and Automation (ICMICA)*, June.

Kumar, S. and Dewan, L. (2022a). Pfoid-smc approach to mitigate the effect of disturbance and parametric uncertainty on the quadcopter. *International Journal of Modelling, Identification and Control*, **40** (4), pp. 343–355.

Kumar, S. and Dewan, L. (2022b). Quadcopter stabilization using hybrid controller under mass variation and disturbances. *Journal of Vibration and Control*.

Kumar, S. and Dewan, L. (2024). Trajectory tracking controller design for quadcopter under disturbances environment: using a hybrid approach. *Cybernetics and Physics*, **13** (3), pp. 248–260.

Le, H., Ngoc, N., and Hong, S. K. (2018). Quadcopter robust adaptive second order sliding mode control based on pid sliding surface. *IEEE Access*, **6**, pp. 66850–66860.

Leal, I. S., Abeykoon, C., and Perera, Y. S. (2021). Design, simulation, analysis and optimization of pid and fuzzy based control systems for a quadcopter. *Electronics*, **10** (18), pp. 2218.

Luchinsky, D. G., Schuet, S. R., and Goebel, K. Dynamics and control of quadcopter in uncertain environment. Incomplete reference.

Luque-Vega, L., Castillo-Toledo, B., and Loukianov, A. G. (2012). Robust block second order sliding mode control for a quadrotor. *Journal of the Franklin Institute*, **349** (2), pp. 719–739.

Modirrousta, A. and Khodabandeh, M. (2015). Adaptive second order terminal backstepping sliding mode for attitude control of quadrotor with external disturbances. *Majlesi Journal of Electrical Engineering*, **9** (2), pp. 51–58.

Nguyen, N. P., Mung, N. X., Thanh, H. L. N. N., Huynh, T. T., Lam, N. T., and Hong, S. K. (2021). Adaptive sliding mode control for attitude and altitude system of a quadcopter uav via neural network. *IEEE Access*, **9**, pp. 40076–40085.

Rabah, M., Rohan, A., Han, Y. J., and Kim, S. H. (2018). Design of fuzzy-pid controller for quadcopter trajectory-tracking. *International Journal of Fuzzy Logic and Intelligent Systems*, **18** (3), pp. 204–213.

Ribeiro, T. T., Conceição, A. G. S., Sa, I., and Corke, P. (2015). Nonlinear model predictive formation control

for quadcopters. *IFAC-PapersOnLine*, **48** (19), pp. 39–44.

Runcharoon, K. and Srichatrapimuk, V. (2013). Sliding mode control of quadrotor. In *2013 International Conference on Technological Advances in Electrical, Electronics and Computer Engineering (TAEECE)*, pp. 552–557.

Sabzevari, D., Kargar, S. M., and Zanjani, S. M. A. (2016). Mathematical modeling and designing pid controller for a quadrotor and optimizing its step response by genetic algorithm. *Majlesi Journal of Electrical Engineering*, **10** (4), pp. 17–24.

Sharma, A. and Lather, J. S. (2024). Synchronization of coupled quadcopters using contraction theory. *Cybernetics and Physics*, **13** (2), pp. 142–151.

Sharma, A. and Lather, J. S. (2025). Gain scheduling of backstepping sliding mode controller using optimized type-1 sugeno fuzzy logic approach for quadcopter. *Aircraft Engineering and Aerospace Technology*. Ahead-of-print.

Usman, M. Quadcopter modelling and control with matlab/simulink implementation. No publication details provided.

Xiong, J. J. and Zheng, E. H. (2014a). Position and attitude tracking control for a quadrotor uav. *ISA Transactions*, **53** (3), pp. 725–731.

Xiong, J. J. and Zheng, E. H. (2014b). Position and attitude tracking control for a quadrotor uav. *ISA Transactions*, **53** (3), pp. 725–731.

Zaeri, A. H., Esmaeilian-Marnani, A., and Noor, S. B. M. (2019). Sliding mode control improvement by using model predictive, fuzzy logic, and integral augmented techniques for a quadrotor helicopter model. *Majlesi Journal of Electrical Engineering*, **13** (4), pp. 25–37.